LA-UR-97-918

CONF-971115--1

Los Alamos National Laboratory is operated by the University of California for the United States Department of Energy under contract W-7405-ENG-36

TITLE: **ON THE INTERFACE INSTABILITY DURING RAPID EVAPORATION IN MICROGRAVITY**

AUTHOR(S): Damir Juric, T-3

SUBMITTED TO: *1997 International Mechanical Engineering Congress and Exposition (ASME), Dallas, Texas, November 16–21, 1997*

Los Alamos National Laboratory
Los Alamos, New Mexico 87545

FORM NO. 836 R4
ST. NO. 2629 5/81

DISCLAIMER

ON THE INTERFACE INSTABILITY DURING RAPID EVAPORATION IN MICROGRAVITY

Damir Juric
Theoretical Division
Los Alamos National Laboratory
Los Alamos, New Mexico

ABSTRACT

The rapid evaporation of a superheated liquid (vapor explosion) under microgravity conditions is studied by direct numerical simulation. The time-dependent Navier-Stokes and energy equations coupled to the interface dynamics are solved using a two-dimensional finite-difference/front-tracking method. Large interface deformations, topology change, latent heat, surface tension and unequal material properties between the liquid and vapor phases are included in the simulations. A comparison of numerical results to the exact solution of a one-dimensional test problem shows excellent agreement. For the two-dimensional rapid evaporation problem, the vapor volume growth rate and unstable interface dynamics are studied for increasing levels of initial liquid superheat. As the superheat is increased the liquid-vapor interface experiences increasingly unstable energetic growth. These results indicate that heat transfer plays a very important role in the instability mechanism leading to vapor explosions. It is suggested that the Mullins-Sekerka instability could play a role in the instability initiation mechanism.

INTRODUCTION

In vapor explosions, extremely rapid evaporation of a liquid at the superheat limit due to sudden depressurization or contact with a hotter surface can lead to destructive accidents (Reid, 1983). Vapor explosions within fluid filled tanks or piping are a particularly serious safety concern in the space environment where energy generation systems for spacecraft depend on the storage and flow of low boiling point cryogenic fluids. Understanding the basic behavior of the liquid-vapor interface during rapid evaporation is the key to addressing this concern.

A basic understanding of explosive bubble growth is hindered by the small spatial scales and the rapidity of the phase change process both of which make it very difficult to obtain the necessary experimental measurements. Furthermore, opportunities for experimental investigation of vapor explosions under microgravity conditions are limited to short duration experiments on Earth or to expensive space flights. Analytical and numerical efforts to understand the processes involved in boiling have focused mainly on simple models of vapor bubble dynamics. An assumed interface shape along with various assumptions concerning surface tension, fluid viscosity and vapor phase velocity and temperature are usually incorporated (Rayleigh, 1917, Plesset and Zwick, 1952, 1954, Mikic, et al, 1970, Dalle Donne and Ferranti, 1975, Lee, 1996, Lee and Nydahl, 1989, Patil and Prusa, 1991).

Several experimental studies involving the superheating of liquid drops in bubble columns have been undertaken to characterize the vapor explosion phenomenon (Shepherd and Sturtevant, 1982, Frost and Sturtevant, 1986, Frost, 1988). The Landau (1944) instability has been proposed as a hydrodynamic mechanism for unstable growth. However, growth rates calculated with this model disagree with the experimental measurements of Shepherd and Sturtevant (1982). Ervin et al. (1992) have observed an interfacial instability on the surface of bubbles in microgravity boiling experiments. They were the first to report observations of this type of interfacial instability in a bulk liquid heated from a solid surface. They believe that the small scale protuberances on the growing bubble's surface greatly increase the liquid-vapor interface surface area which then results in rapid evaporation and the creation of more protuberances. Considering these experimental observations, Lee and Merte (1996), propose that the interfacial in-

stability includes a combination of thermal and hydrodynamic mechanisms. They present a planar instability model including heat transfer that reasonably predicts the occurrence of the explosive bubble growth as well as the instability wavelength. Other studies have been conducted on plane surfaces (Prosperetti and Plesset, 1984, Higuera, 1987), however, the exact nature of the instability mechanism is still an unsettled issue.

The complete phase change problem is highly dependent on the simultaneous coupling of many effects none of which can typically be ignored. The modeling of mass, momentum and energy transport must include surface tension, latent heat, interphase mass transfer, discontinuous material properties and complicated liquid-vapor interface dynamics. Only recently have numerical methods begun to offer the promise of helping to provide accurate predictions of the detailed small scale physical processes involved in phase change. Welch (1995) has made significant progress in using a two-dimensional, moving mesh, finite volume method to solve the mass, momentum and energy equations for liquid-vapor flows with phase change. However, his method is restricted to flows with only small distortion of the liquid-vapor interface. Son (1996) and Son and Dhir (1995) use a moving mesh finite difference method for two-dimensional simulations of phase change. Using grid generation techniques they study the heat transfer and interface behavior in film boiling up to the point of bubble departure.

In a previous paper, Juric and Tryggvason (1995) developed a general two-dimensional front-tracking method for liquid-vapor flows with phase change that can handle large interface deformations and topology change. This method was used for studying a variety of phase change problems (Juric and Tryggvason, 1996a, Juric, 1996) including film boiling from a flat heated surface with vapor bubble pinch off (Juric and Tryggvason, 1996b, 1996c) We use this method here to present calculations of explosive boiling of a superheated liquid in microgravity. The front-tracking technique enables the simulation of problems with complex motion of the liquid-vapor interface including large interface deformations and topology change. The effects of interphase mass transfer, latent heat, surface tension and unequal material properties between liquid and vapor phases are also included. The method is based on a finite difference approximation of the Navier-Stokes and energy equations and an explicit tracking of the phase boundary. The method is an extension of techniques developed for multifluid flows without phase change in both two- and three-dimensions by Unverdi and Tryggvason (1992a, 1992b). The multifluid code has been used to investigate the collision of drops (Nobari et al, 1996, Nobari and Tryggvason, 1996), thermal migration of drops (Nas and Tryggvason, 1993), the collapse of cavitation bubbles (Yu et al, 1995) and the motion of hundreds of interacting bubbles (Esmaeeli and Tryggvason, 1996).

The next section of this paper is devoted to the mathematical formulation of the liquid-vapor phase change problem and a brief description of the front-tracking method presented in Juric and Tryggvason (1995) and Juric (1996). In the third section we present results from a validation test of the method. We also focus on two-dimensional simulations of rapid evaporation in superheated liquids and study the effect of increasing levels of initial superheat. In the fourth section we discuss some conclusions from this study.

FORMULATION

The liquid-vapor phase change problem involves combined fluid flow and heat transfer and thus requires the solution of the Navier-Stokes and energy equations. Note that in two-phase flow, additional terms appear in these equations due to the phase change and the fact that the interface is no longer a material interface. The fluid velocity at the interface and the interface velocity are unequal.

A single set of governing equations is written for both phases. This local, single field formulation incorporates the effect of the interface on the governing equations as sources which act only at the interface. Mass transfer across the interface and momentum as well as energy sources at the interface are taken into account. Kataoka (1985) shows that this local, single field representation is equivalent to the local, separate phase formulations of Ishii (1975) and Delhaye (1974). They formulate the phase change problem in terms of variables for each phase with appropriate jump conditions at the moving phase interface. Those local, separate phase formulations form a fundamental basis for all averaged models of two-phase mixtures.

Here the single field, local formulation is used. The material properties are considered to be constant but not generally equal for each phase. They can be written for the entire domain and advected using an indicator function, $I(\mathbf{x},t)$. This function is determined from the known position of the interface and has the value 1 in the vapor phase and 0 in the liquid phase. The values of the material property fields at every location are then given by:

$$b(\mathbf{x},t) = b_l + (b_v - b_l)\, I(\mathbf{x},t)\,, \qquad (1)$$

where the subscripts v and l refer here to the vapor and

liquid phases respectively and b stands for density, p, specific volume, $\hat{v} = 1/p$, viscosity, μ, specific heat, c or thermal conductivity, k. To simplify the presentation of the formulation that follows we will assume that $c_l = c_v$. The formulation for $c_l \neq c_v$ is only slightly more involved and is given in Juric (1996).

The momentum equation is written for the entire flow field and the forces due to surface tension are inserted at the interface as body forces which act only at the interface. In conservative form this equation is

$$\frac{\partial \mathbf{w}}{\partial t} + \nabla \cdot (\mathbf{wu}) = -\nabla P - p\mathbf{g} + \nabla \cdot \mu \left(\nabla \mathbf{u} + \nabla \mathbf{u}^T\right) + \int_{\mathcal{A}} \frac{\partial (\gamma \mathbf{t})}{\partial s} \delta (\mathbf{x} - \mathbf{x}_f)\, d\mathcal{A} . \quad (2)$$

Here $\mathbf{u}$ is the fluid velocity field, $\mathbf{w} = p\mathbf{u}$ is the mass flux and P is the pressure. The last term on the right side accounts for surface tension acting on the interface $\mathcal{A}$. $\delta (\mathbf{x} - \mathbf{x}_f)$ is a three-dimensional delta function that is non-zero only at the interface where $\mathbf{x} = \mathbf{x}_f$. γ is the surface tension coefficient and κ is twice the mean curvature. Thermocapillary forces acting in a direction, $\mathbf{t}$, tangential to the interface could arise from variation of the surface tension with temperature, but this effect is neglected here.

The conservation of mass equation is also written for the entire flow field:

$$\frac{\partial p}{\partial t} + \nabla \cdot \mathbf{w} = 0 . \quad (3)$$

The time derivative of the density can be rewritten in a more useful form since the density at each point in the domain, Eq. (1), depends only on the indicator function which is determined by the known interface location. Using the indicator function, $I(\mathbf{x}, t)$, to represent the interface, the kinematic equation for a surface moving with velocity, $\mathbf{V}$, is

$$\frac{\partial I}{\partial t} = -\mathbf{V} \cdot \nabla I . \quad (4)$$

Since I is constant except in a local region near the interface, the gradient of I can be written as a local surface integral:

$$\nabla I = \int_{\mathcal{A}} \mathbf{n} \delta (\mathbf{x} - \mathbf{x}_f)\, d\mathcal{A} . \quad (5)$$

Using Eqs. (4), (5) and Eq. (1) for the density, the conservation of mass, Eq. (3), can be rewritten as:

$$\nabla \cdot \mathbf{w} = \int_{\mathcal{A}} (p_v - p_l)\, \mathbf{V} \cdot \mathbf{n} \delta (\mathbf{x} - \mathbf{x}_f)\, d\mathcal{A} \quad (6)$$

The thermal energy equation is (Bird, 1960)

$$\frac{\partial}{\partial t} (pcT) + \nabla \cdot (\mathbf{w}cT) = \nabla \cdot K \nabla T - pT \left(\frac{\partial P}{\partial T}\right)_{\hat{v}} \frac{D\hat{v}}{Dt} \quad (7)$$

where T is the temperature and viscous dissipation has been neglected. Using Eqs. (1) and (4) the material derivative, $D\hat{v}/Dt$, can be written as (Aris, 1962):

$$\frac{D\hat{v}}{Dt} = (\hat{v}_v - \hat{v}_l)\, (\mathbf{u} - \mathbf{V}) \cdot \nabla I . \quad (8)$$

In addition, the Clausius-Clapeyron relation along the pressure-temperature saturation curve gives:

$$\left(\frac{\partial P}{\partial T}\right)_{\hat{v}} = \left(\frac{dP}{dT}\right)_{\text{sat}} = \frac{L}{(\hat{v}_v - \hat{v}_l)\, T_f} \quad (9)$$

where $T_f = T(\mathbf{x}_f(t))$ is the interface temperature and L is the latent heat measured at the reference equilibrium vaporization temperature, T_v.

Using Eqs. (8), (9) and (5), the thermal energy equation, Eq. (7), can be rewritten as:

$$\frac{\partial}{\partial t} (pcT) + \nabla \cdot (\mathbf{w}cT) = \nabla \cdot K \nabla T + \int_{\mathcal{A}} L\, (p\mathbf{V} - \mathbf{w}) \cdot \mathbf{n} \delta (\mathbf{x} - \mathbf{x}_f)\, d\mathcal{A} . \quad (10)$$

The last term on the right accounts for liberation or absorption of latent heat at the interface.

It is important to recognize that the single field formulation (Eqs. (2), (6) and (10)) naturally incorporates the correct mass, momentum and energy balances across the interface since integration of these equations across the interface directly yields the jump conditions derived in the local instant formulation for two-phase systems given by Delhaye (1974) and Ishii (1975). We assume that the interface is thin and massless and that the bulk fluids are incompressible. In the energy equation, viscous dissipation and kinetic energy contributions from the product of the fluid velocity at the interface and the interface velocity are neglected. Contributions to the source term in the energy equation from interface stretching are usually small compared with the latent heat and are neglected.

To complete the formulation a condition on the temperature at the phase change interface must be specified. In recent studies on interface instability during phase change, Huang and Joseph (1992, 1993) point out that the correct condition for the temperature at a phase change boundary is not known and is still an unresolved physical issue. They note that thermodynamic equilibrium (the Clausius-Clapeyron relation, Eq. (9))

excludes thermal equilibrium (continuity of temperature at the interface, $[T] = 0$). Typically it is assumed that the vapor and liquid temperatures at the interface are equal and the value of this interface temperature determined by the Clausius-Clapeyron relation for the saturation value appropriate to the pressure in the vapor. But since the pressures on either side of the interface are generally not equal the liquid temperature at the interface is then not given by the Clausius-Clapeyron relation. Thus the liquid at the interface is not in thermodynamic equilibrium.

For the numerical calculations in this work, thermal equilibrium at the interface, $[T] = 0$ is assumed, but not thermodynamic equilibrium. The value of the interface temperature, T_f, is found using a slight variation of the interface temperature condition derived by Alexiades (1993) from a careful consideration of the equilibrium Clausius-Clapeyron relation for a curved interface:

$$T_f - T_v - \frac{\gamma T_v}{\rho_l L}\kappa + \frac{T_v}{L}\left(\frac{1}{\rho_l} - \frac{1}{\rho_v}\right)(P_v - P_\infty) + \frac{(\rho \mathbf{V} - \mathbf{w})\cdot \mathbf{n}}{\varphi} = 0\,, \qquad (11)$$

where P_∞ and P_v are the ambient pressure and the pressure at the interface in the vapor respectively. The last term on the left side of this equation is intended to model the thermodynamic nonequilibrium nature of the phase change process through a molecular kinetic parameter, φ. It represents a slight deviation from the equilibrium Clausius-Clapeyron relation. (This nonequilibrium term is not included in Alexiades and Solomon (1993).) Here the molecular kinetic effects are assumed to be linearly proportional to the interface temperature.

The set of equations (1), (2), (6), (10) along with the interface temperature condition, Eq.(11) are solved using the finite difference/front tracking method described in Juric and Tryggvason (1995) and Juric (1996). Briefly, these equations are solved iteratively for the correct interface velocity, V, that will satisfy the interface temperature condition, Eq.(11). For the spatial discretization, we use the MAC method of Harlow and Welch (1965) with a staggered mesh. Chorin's (1968) projection algorithm with a modification to account for phase change is used for the time integration. The interface is explicitly represented by separate, non-stationary computational points connected to form a one-dimensional front which lies within the two-dimensional stationary mesh. These points are used to calculate interface normals, curvature and in the construction of the indicator function.

RESULTS

Comparison with an Exact Solution

We tested the numerical method by comparing numerical results with the exact solution of a simple one-dimensional problem. The one-dimensional problem consists of a heat flux, q_w, applied to the bottom of a rigid wall at $y = 0$. The domain contains a liquid $0 \lesssim y \lesssim 0.5$ below its vapor $0.5 \lesssim y \lesssim 1$. The top of the domain at $y = 1$ remains open to allow for the vapor to exit due to fluid expansion at the interface. The density ratio is set to $\rho_l/\rho_v = 2$. All other material properties are equal. To make the problem dimensionless we scale lengths by a reference length, l, velocities by a reference velocity, U_o, the heat flux by $\rho_l L$ and the pressure (measured from ambient, $P_\infty = 0$) by $\rho_l U_o^2$. For this calculation $q_w = 0.05$ and there is no gravity.

For slow interface motion the heat flux in the liquid remains approximately constant and the interface moves at a steady velocity. Then exact steady-state solutions for the interface velocity, vertical fluid velocity and pressure are:

$$V = -q_w\,, \quad u_l = 0\,, \quad u_v = \left(1 - \frac{\rho_l}{\rho_v}\right)V\,,$$

$$P = \left(\frac{\rho_l}{\rho_v} - 1\right)V^2\,.$$

After a short initial transient, the calculated interface velocity smoothly asymptotes to the correct steady state value of the exact solution, $V = -0.05$. (Negative since the interface moves downward.)

Results for the vertical fluid velocity, Fig. (1), and pressure, Fig. (2), are shown at $t = 1.4$ for three grid resolutions, 10 x 10, 20 x 20 and 40 x 40. Even at crude resolutions the numerical results in the bulk liquid and vapor are in excellent agreement with the exact solution. However the results at the interface are of greater interest. The exact solution is perfectly discontinuous while the numerical interface has a finite thickness which decreases as the resolution increases. This behavior nicely demonstrates the convergence with increasing grid resolution of the front tracking approach to modeling discontinuities across an interface. The front tracking method inherently distributes the effects of the interface smoothly to mesh points in a localized region near the interface. Thus as the resolution increases these effects become sharper and more localized near the interface. Higher density ratios, up to $\rho_l/\rho_v = 1000$ were also tested and the results were equally as good.

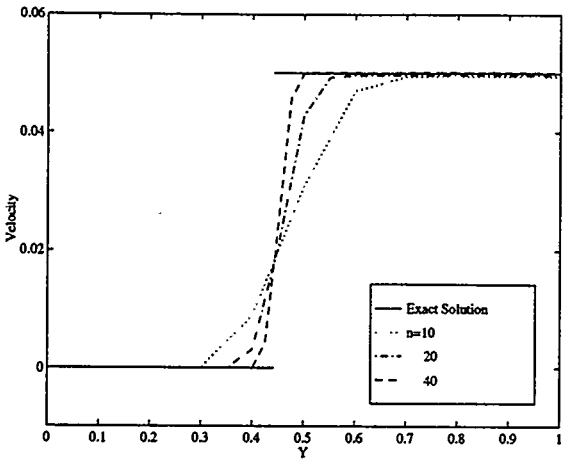

Figure 1: Comparison of exact and numerical fluid velocity for one-dimensional boiling. The numerical results in the bulk liquid and vapor are in excellent agreement with the exact solution. The exact solution is perfectly discontinuous at the interface while the numerical interface has a finite thickness which decreases as the resolution increases. This behavior nicely demonstrates the convergence with increasing grid resolution of the front tracking approach to modeling discontinuities across an interface.

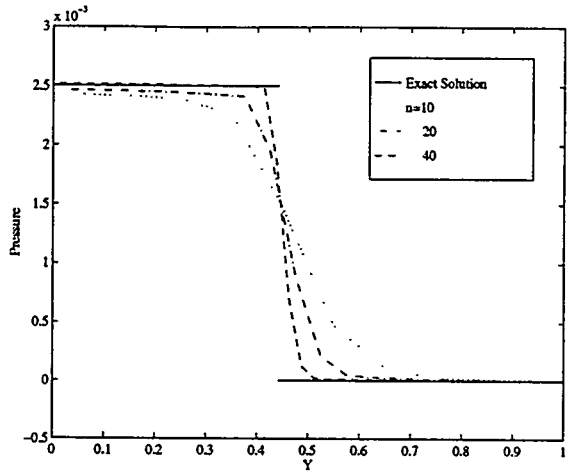

Figure 2: Comparison of exact and numerical pressure for one-dimensional boiling. Again the agreement is excellent at the highest resolution.

Vapor Explosion

Here we present the results of two-dimensional simulations of evaporation from a superheated liquid under microgravity (g = 0) conditions. The governing equations and boundary conditions can be made dimensionless by scaling length by a suitable length scale, l, time by $p_l c_l l^2/K_l$ and velocity by, $K_l/p_l c_l l$. The resulting nondimensional parameters are the Prandtl number, $Pr = \mu_l c_l/K_l$, the Jakob number, $Ja = p_l c_l (T_\infty - T_v)/p_v L$, a "Weber" number, $We = K_l^2/p_l c_l^2 \gamma l$, a capillary parameter, $\sigma = c_l T_v \gamma/p_v L^2 l$ and a dimensionless nonequilibrium parameter, $\vartheta = K_l/p_v L \varphi l$. In addition to these we must specify the 4 ratios of the material properties between the liquid and the vapor.

In the simulations shown in figure (3) we follow the evolution of an initially nearly circular interface in a box of dimensions 1 x 1. The domain is periodic in the horizontal direction and the bottom wall is rigid. To allow for expansion due to evaporation we let the ambient fluid exit at the top boundary. We specify a pressure condition at the top boundary of $P = 0$. The temperature field is initially set to a uniform initial superheat, $Ja = 0$, in the vapor and $Ja = 1, 2, 3$ in the liquid for Figs. (3)a, b and c respectively. The grid resolution is 200 x 200 for Fig. (3)a and b while we have used a higher resolution of 300 x 300 for Fig. (3)c in order to resolve the details of the vapor bubble microstructure. The following nondimensional parameters were used:

$$\frac{p_l}{p_v} = 10, \quad \frac{\mu_l}{\mu_v} = 40, \quad \frac{K_l}{K_v} = 20, \quad \frac{c_l}{c_v} = 1,$$

$$Pr = 1, \quad We = 20, \quad \sigma = 0.001, \quad \vartheta = 0.002$$

Depending on the particular fluid and conditions these values are realistic. For comparison, the properties of saturated fluids are given by Maddox (1983). For cryogenic fluids such as hydrogen and oxygen, the values of the liquid to vapor density ratios are roughly 54 and 253 respectively at a pressure of 1 atm. While at about 9 atm these ratios are approximately 4 and 28 for hydrogen and oxygen respectively. These values are typical of cryogenic fluids and refrigerants while for water the ratio is roughly an order of magnitude higher, 1600 and 147 at 1 atm and 12 atm respectively.

At 1 atm the viscosity ratio of liquid to vapor for these substances is in the range of 20 to 30, the thermal conductivity ratio in the range 7 to 30 and the specific heat ratio in the range 0.8 to 2. The Prandtl number, Pr, ranges from about 1 to 2 and for a Weber number of $We = 20$ the length scale for the calculations is roughly 10^{-4}m. At $Ja = 1$ and $p_l/p_v = 10$, the dimensional superheat is about 2, 6 and 18 Kelvin for hydrogen, oxygen and water respectively.

The initial interface at $t = 0$ is shown in the center of each frame of Fig. (3). In order to trigger

unstable growth, this initial interface is specified as a slightly perturbed circle with eight symmetric lobes. Each frame also shows the interface at a later time: $t =$ 0.016,0.004,0.00032 respectively for Figs. (3)a, b and c. As the superheat is increased the interface grows more rapidly and with more convolutions while the wavelength of the surface instability decreases. As we would expect the most rapid and unstable growth occurs in Fig. (3)c, at the largest of the three superheats, $Ja = 3$. There we see a similar fine scale wrinkling of the bubble surface as observed in the microgravity experiments of Ervin et al (1992) and the bubble column experiments of Shepherd and Sturtevant (1982).

Figs. (4) and (5) show the growth in interface length and vapor volume fraction with time respectively for the three superheats in Fig. (3). The vapor volume growth rate for $Ja = 3$ is about an order of magnitude greater than that of $Ja = 1$. The interface length for the smoothest bubble at $Ja = 1$ grows nearly according to the $\sqrt{t}$ growth expected of a circular bubble. Consistent with this, the vapor volume (area in 2d) fraction grows linearly with time. However, for higher superheats both the interface length and the vapor volume fraction grow linearly with time indicating that during unstable growth the average radius of the bubble grows linearly. This result is in agreement with the measurements of Shepherd and Sturtevant (1982), Ervin et al (1992) and Lee and Merte (1996). For unstable bubble growth they measured a nearly linear increase in the effective bubble radius with time. This result also lends support to the theory that convolutions or wrinkles of the surface increase its area and enhance the rate of heat transfer and evaporation thus leading to explosive growth.

In figure (6) temperature and velocity fields are plotted for the $Ja = 2$ calculation of Fig. (3). The shades of gray indicate the temperature with black corresponding to a nondimensional temperature of -0.5 and white 2.0. The thicker black line is the liquid/vapor interface. The velocity vectors indicate that there is a general flow of liquid outward, away from the expanding bubble. The flow in the vapor bubble is more complex due to the inflow of vapor from the interface. The velocity vectors in the core of the bubble show a general upward motion of the entire bubble. This upward motion is consistent with the constraints of the rigid bottom wall and the outward flow of ambient liquid at the top boundary. Note the discontinuity of the fluid velocity at the liquid-vapor interface due to the transfer of mass across the interface.

We observe that the process of evaporation from a superheated liquid is analogous to the well studied prob-

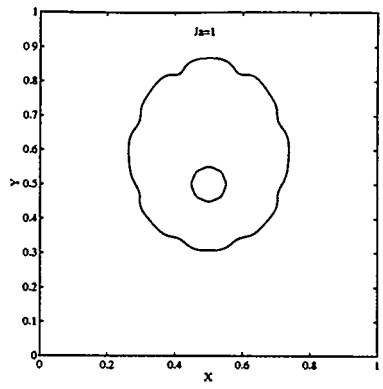

(a)

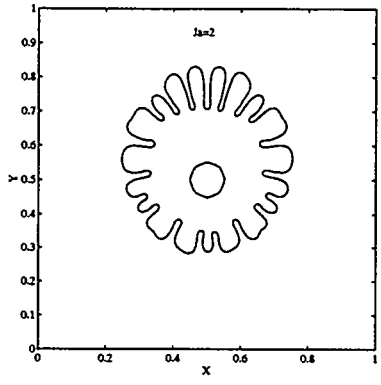

(b)

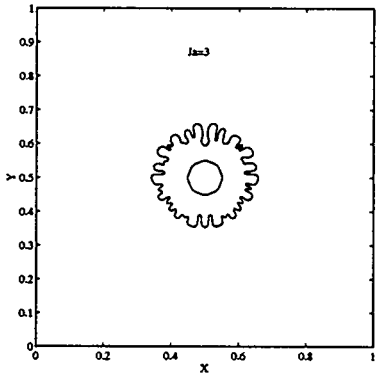

(c)

Figure 3: The growth of interface instabilities on a bubble growing in a superheated liquid in microgravity. As the superheat is increased the interface growth is more rapid and more unstable. The initial interface is shown as the nearly circular shape in the center of the figure. Also shown the are the interfaces at times $t = 0.016$,0.004 and 0.00032 for $Ja = 1$, 2 and 3 respectively.

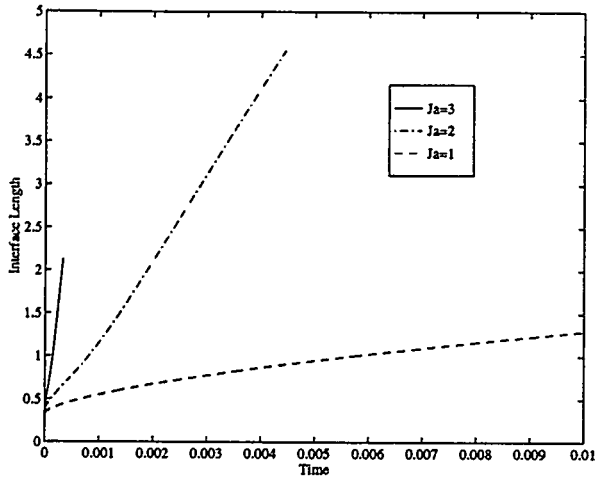

Figure 4: The interface length vs. time for the three superheats shown in Fig. (3).

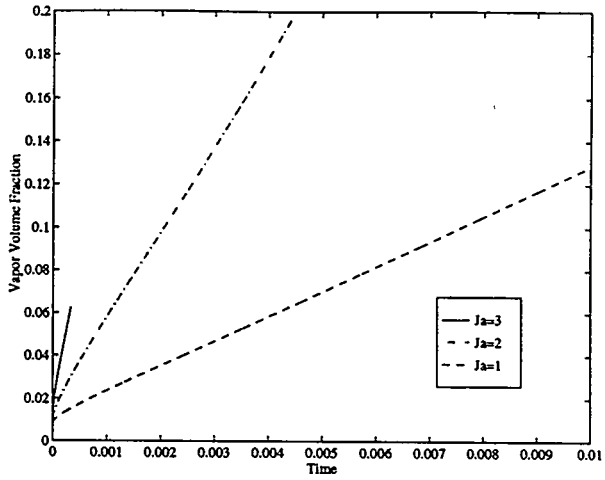

Figure 5: The vapor volume fraction vs. time for the three superheats shown in Fig. (3).

lem of unstable solidification from a supercooled melt which results in the growth of dendritic structures in the solid. (See Juric, 1996a for a brief review of this literature.) In unstable solidification heat is conducted away from the solid-liquid interface through the liquid. Any local protrusion of the interface that extends into the liquid will be enhanced since the magnitude of the temperature gradient at the protrusion is greater than that at adjacent portions of the interface. The process is inherently unstable and the protrusion will grow until constrained by surface tension effects. In solidification, the onset of growth of these protrusions is described by the Mullins-Sekerka instability mechanism (Mullins and Sekerka, 1964). Eventually this instability results in the formation of dendrites which are observed to grow in length at a constant speed.

This analogy suggests that the Mullins-Sekerka mechanism is responsible for at least part of the observed small scale interfacial instability in vapor explosions. This type of instability would be present regardless of the density ratio and would depend primarily on the liquid superheat and surface tension. Certainly, other instability mechanisms are also present in vapor explosions due to the hydrodynamic effect of vapor expansion upon evaporation. Interestingly both radially growing dendritic structures and unstably growing vapor bubbles are observed to increase their effective radii linearly with time.

CONCLUSIONS

We have shown results from two-dimensional direct numerical simulations of rapid evaporation in a superheated liquid under microgravity conditions. The simulations of rapid evaporation in sufficiently superheated liquids demonstrate the formation of highly convoluted unstable interfaces. These convolutions or wrinkles of the surface increase its area and enhance the rate of heat transfer and evaporation thus leading to explosive growth. Thus it is clear that heat transfer plays a very important role in the instability mechanism leading to vapor explosions and future work will investigate this effect in greater detail. We propose that the onset of instability in rapid bubble growth can in part be explained by the well known Mullins-Sekerka interface instability mechanism in unstable solidification.

The simulations in this paper were motivated by the observations of interface instability in microgravity boiling experiments (Ervin et al, 1992). Although the conditions are not exactly the same, our preliminary simulations show the qualitatively correct features of interface instability in microgravity boiling. Further work is underway to develop a quantitative fully three-dimensional comparison with the microgravity boiling experiments.

Acknowledgments

This work was supported in part by the NASA Microgravity Fluid Physics Program, NSF Grant CTS-9503208 and by NASA Graduate Student Fellowship NGT-51070. I would also like to acknowledge helpful discussions with Dr. Ho Sung Lee and Prof. Herman Merte of the University of Michigan and Drs. Jerry Brackbill, Doug Kothe and Rick Rauenzahn of the Los

Alamos National Laboratory.

BIBLIOGRAPHY

Alexiades, V., and Solomon, A. D., 1993, *Mathematical Modeling of Melting and Freezing Processes* (Hemisphere, Washington, D.C.), p. 92.

Aris, R., 1962, *Vectors, Tensors and the Basic Equations of Fluid Mechanics* (Dover, New York), p. 79.

Bird, R. B., Stewart, W. E. and Lightfoot, E. N., 1960, *Transport Phenomena,* (Wiley, New York), p. 323.

Chorin, A. J., 1968, "Numerical Solution of the Navier-Stokes Equations", *Mathematics of Computation*, **22**, pp. 745-762.

Dalle Donne, M., and Ferranti, M. P., 1975, "The Growth of Vapor Bubbles in Superheated Sodium", *Int. J .Heat and Mass Transfer*, Vol. 18, pp. 477-493.

Delhaye, J. M., 1974, "Jump Conditions and Entropy Sources in Two-Phase Systems. Local Instant Formulation", *Int. J. Multiphase Flow*, Vol 1, pp. 395.

Ervin, J. S., Merte, Jr. H., Keller, R. B., and Kirk, K., 1992, "Transient Pool Boiling in Microgravity," *Int. J. Heat Mass Transfer*, Vol. 35, pp.659-674.

Esmaeeli, A. and Tryggvason, G., 1996, "An Inverse Energy Cascade in 2-Dimensional Low Reynolds Number Bubbly Flows," *J. Fluid Mech.*, **314**, pp. 315-330.

Frost, D., 1988, "Dynamics of Explosive Boiling of a Droplet," *Phys. Fluids*, Vol. 31, pp. 2554-2561.

Frost, D. and Sturtevant, B., 1986, "Effects of Ambient Pressure on the Instability of a Liquid Boiling Explosively at the Superheat Limit," *J. Heat Transfer*, Vol. 108, pp. 418-424.

Harlow, F. H. and Welch, J. E., 1965, "Numerical Calculation of Time-Dependent Viscous Incompressible Flow of Fluid with Free Surface", *Physics of Fluids*, **8**, pp. 2182-2189.

Higuera, F. J., 1987, "The Hydrodynamic Stability of an Evaporating Liquid," *Phys. Fluids*, **30**, pp. 679-686.

Huang, A. and Joseph, D. D., 1992, "Instability of the Equilibrium of a Liquid Below its Vapour Between Horizontal Heated Plates," *J. Fluid Mech.*, **242**, pp. 235-247.

Huang, A. and Joseph, D. D., 1993, "Stability of Liquid-Vapor Flow Down an Inclined Channel with Phase Change," *Int. J. Heat Mass Transfer*, **36**, pp. 663-672.

Ishii, M., 1975, *Thermo-Fluid Dynamic Theory of Two-Phase Flow*, Eyrolles, Paris.

Juric, D., 1996, "Computations of Phase Change," *Ph.D. Dissertation*, The University of Michigan.

Juric, D., and Tryggvason, G., 1995, "A Front-Tracking Method for Liquid-Vapor Phase Change," in *Advances in Numerical Modeling of Free Surface and Interface Fluid Dynamics*, FED-Vol. 234, ASME, pp. 141-148.

Juric, D., and Tryggvason, G., 1996a, "A Front-Tracking Method for Dendritic Solidification," *J. Comp. Phys*, Vol. 123, pp. 127-148.

Juric, D. and Tryggvason, G., 1996b, "Computations of Film Boiling," in *Advances in Numerical Modeling of Free Surface and Interface Fluid Dynamics*, FED-Vol. 238, (ASME, New York) pp. 341-347.

Juric, D. and Tryggvason, G., 1996c, "Direct Numerical Simulations of Flows with Phase Change," AIAA Technical Report, 96-0857.

Kataoka, I. 1985, "Local Instant Formulation of Two-Phase Flow", Technical Report Institute of Atomic Energy, Kyoto University, Kyoto, Japan, Vol. 203, pp. 1-33.

Landau, L. 1994, "On the Theory of Slow Combustion," *Acta Physicochemica U.S.S.R.*, **19**, pp. 77-85.

Lee H. S. and Merte, Jr., H., 1996, "The Origin of the Dynamic Growth of Vapor Bubbles Associated with Vapor Explosions," in *Heat Transfer in Microgravity Systems*, HTD-Vol. 332, ASME.

Lee, R. C., and Nydahl, J. E., 1989, "Numerical Calculation of Bubble Growth in Nucleate Boiling from Inception through Departure", *J. Heat Transfer*, Vol. 111, pp. 474-479.

Maddox, R. N., 1983, "Properties of Saturated Fluids," in *Heat Exchanger Design Handbook*, (Hemisphere, New York).

Mikic, B. B., Rohsenow, W. M., and Griffith, P., 1970, "On Bubble Growth Rates", *Int. J. Heat and Mass Transfer*, Vol. 13, pp. 657-666.

Mullins, W. W., and Sekerka, R. F., 1964, "Stability of a Planar Interface During Solidification of a Dilute Binary Alloy," *J. Appl. Phys.*, Vol. 35, pp. 444-451.

Nas, S., and Tryggvason, G., 1993, "Computational Investigation of Thermal Migration of Bubbles and Drops", *Proceedings ASME Winter Annual Meeting, AMD 174/FED 175 Fluid Mechanics Phenomena in Microgravity*, D.A. Siginer et al., ed., pp. 71-83.

Nobari, M.R., Jan, Y.-J., and Tryggvason, G., 1996, "Head on Collision of Drops - A Numerical Investigation", *Phys. Fluids*, **8**, pp. 29-42.

Nobari, M.R., and Tryggvason, G., 1996, "Numerical Simulations of Three-Dimensional Drop Collisions," *AIAA Journal*, **34**, pp. 750-755.

Patil, R. K., and Prusa, J., 1991, "Numerical Solutions for Asymptotic, Diffusion Controlled Growth of a Hemispherical Bubble on an Isothermally Heated Sur-

face", *Experimental/Numerical Heat Transfer in Combustion and Phase Change*, ASME HTD, Vol. 170, pp. 63-70.

Plesset, M. S., and Zwick, S. A., 1952, "A Nonsteady Heat Diffusion Problem with Spherical Symmetry", *J. Appl. Phys.*, Vol. 23, p. 95.

Plesset, M. S. and Zwick, S. A., 1954, "The Growth of Vapor Bubbles in Superheated Liquids," *J. Appl. Phys.*, **25**, pp. 493-500.

Prosperetti, A. and Plesset, M. S., 1978, "Vapor Bubble Growth in a Superheated Liquid," *J. Fluid Mech.*, Vol. 85, pp. 349-368.

Prosperetti, A. and Plesset, M. S., 1984, "The Stability of an Evaporating Liquid Surface," *Phys. Fluids*, **27**, pp. 1590-1602.

Rayleigh, 1917, "On the Pressure Developed in a Liquid During the Collapse of a Spherical Cavity", *Phil. Mag.*, Vol. 34, pp. 94-98.

Reid, R. C., 1983, "Rapid Phase Transitions from Liquid to Vapor," *Adv. Chem. Eng.*, Vol. 12, pp. 105-208.

Shepherd, J. E., and Sturtevant, B., 1982, "Rapid Evaporation at the Superheat Limit," *J. Fluid Mech.*, Vol. 121, pp. 379-402.

Son, G., 1996, "Numerical Simulation of Nonlinear Taylor Instability with Application to Film Boiling, Melting and Sublimation," *Ph.D. Dissertation*, The University of California, Los Angeles.

Son, G. and Dhir, V. K., 1995, "Two-Dimensional Numerical Simulation of Saturated Film Boiling on a Horizontal Surface," in *Proc. ASME/JSME Thermal Engineering Joint Conf.*, edited by L. S. Fletcher and T. Aihara (ASME, New York), pp. 257-264.

Unverdi, S. O., and Tryggvason, G., 1992a, "Computations of Multi-fluid Flows", *Physica D*, Vol. 60, pp. 70-83.

Unverdi, S. O., and Tryggvason, G., 1992b, "A Front-Tracking Method for Viscous, Incompressible, Multi-fluid Flows", *J. Computational Physics*, Vol. 100, pp. 25-37.

Welch, S. W. J., 1995, "Local Simulation of Two-Phase Flows Including Interface Tracking with Mass Transfer," *J. Comp. Phys.*, Vol. 121, pp. 142-154.

Yu, P.-W., Ceccio, S. L. and Tryggvason, G., 1995, "The Collapse of a Cavitation Bubble in Shear Flows - A Numerical Study," *Phys. Fluids*, **7**, pp. 2608-2616.

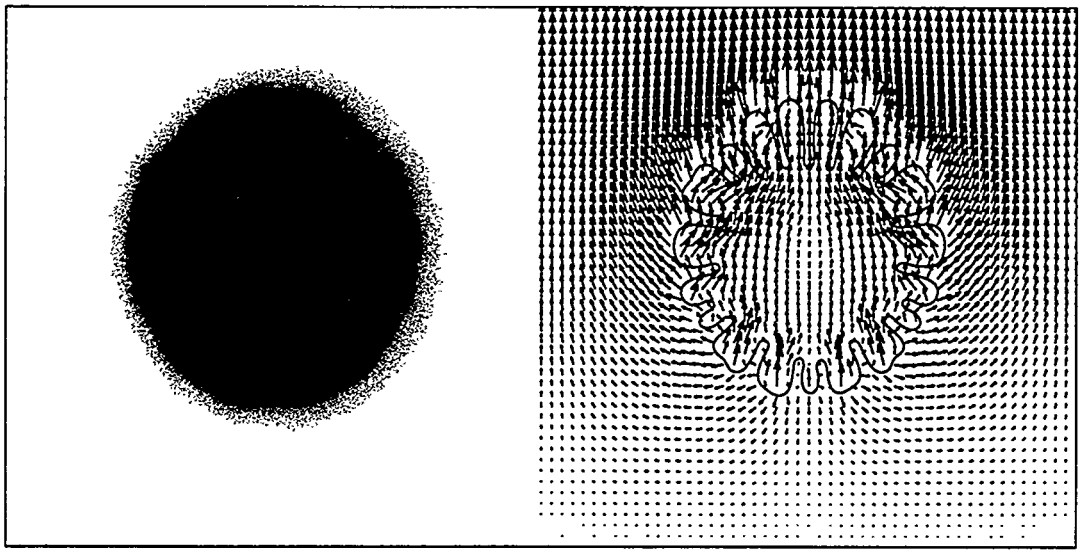

Figure 6: The temperature and velocity fields for the $Ja = 2$ calculation of Fig. (3). The shades of gray indicate the temperature with black corresponding to a nondimensional temperature of -0.5 and white 2.0. The thicker black line is the liquid/vapor interface. The velocity vectors indicate that there is a general flow of liquid outward, away from the expanding bubble. The velocity vectors in the core of the bubble show a general upward motion of the entire bubble. This upward motion is consistent with the constraints of the rigid bottom wall and the outward flow of ambient liquid at the top boundary. Note the discontinuity of the fluid velocity at the liquid-vapor interface due to the transfer of mass across the interface.